Helix-constraints and amino acid substitution in GLP-1 increase cAMP and insulin secretion but not beta-arrestin 2 signaling

Fabien Plisson,[†¶] Timothy A. Hill,[†¶] Justin M. Mitchell,[†] Huy N. Hoang,[†] Aline D. de Araujo,[†] Weijun Xu,[†] Adam Cotterell,[†] David J. Edmonds,[‡] Robert V. Stanton,[‡] David R. Derksen,[#] Paula M. Loria,[#] David A. Griffith,[‡] David A. Price,[‡] Spiros Liras[‡] and David P. Fairlie[†]**

[†]Division of Chemistry and Structural Biology, Institute for Molecular Bioscience, The University of Queensland, St. Lucia, QLD 4072, Australia

[‡]Worldwide Medicinal Chemistry, Cardiovascular, Metabolic & Endocrine Diseases Research Unit, Pfizer Inc., Cambridge, Massachusetts 02140, United States

[#] Pharmacokinetics, Dynamics and Metabolism, Pfizer Inc., Groton, CT 06340, United States

* Corresponding authors. T: (617) 3346 298. F: (617) 3346 2101. E: d.fairlie@imb.uq.edu.au; Tel: (617) 3346 297. Fax: (617) 3346 2101. E: t.hill@imb.uq.edu.au

[¶] Contributed equally.

ABSTRACT

Glucagon-like peptide (GLP-1) is an endogenous hormone that induces insulin secretion from pancreatic islets and modified forms are used to treat diabetes mellitus type 2. Understanding how GLP-1 interacts with its receptor (GLP-1R) can potentially lead to more effective drugs. Modeling and NMR studies of the N-terminus of GLP-1 suggest a β-turn between residues Glu9-Phe12 and a kinked alpha helix between Val16-Gly37. N-terminal turn constraints attenuated binding affinity and activity (compounds **1-8**). Lys-Asp (i, i+4) crosslinks in the middle and at the C-terminus increased alpha helicity and cAMP stimulation without much effect on binding affinity or beta-arrestin 2 recruitment (compounds **9-18**). Strategic positioning of helix-inducing constraints and amino acid substitutions (Tyr16, Ala22) increased peptide helicity and produced ten-fold higher cAMP potency (compounds **19-28**) over GLP-1(7-37)-NH_2. The most potent cAMP activator (compound **23**) was also the most potent inducer of insulin release.

INTRODUCTION

Class B G–protein coupled receptors (GPCRs) are cell surface proteins that mediate numerous physiological functions including those implicated in diabetes, osteoporosis, cardiovascular, neurodegenerative and psychiatric diseases.[1] Glucagon-like peptide-1 receptor (GLP-1R) is the class B GPCR for the hormone glucagon-like peptide (GLP-1). Peptide analogues of this hormone are important agents for the treatment of type 2 diabetes mellitus (T2D).[2] T2D is characterized by hyperglycaemia caused by insulin resistance or defective insulin secretion, with obesity a primary contributing factor to the disease.[3] GLP-1 has two endogenous peptide forms, GLP-1(7-36)-NH_2 and GLP-1(7-37)-OH, that are released from intestinal L cells in response to nutrient sensing. A close analogue GLP-1(7-37)-NH_2 (Figure 1A) is an equipotent analogue of these native forms.[4] Activation of GLP-1R on pancreatic β-cells potentiates glucose-stimulated insulin secretion, insulin gene transcription, β-cell proliferation and inhibition of β-cell apoptosis;[5] all considered desirable for effectively treating T2D. GLP-1 activates GLP-1R in multiple organs with important roles in normal physiology, including neurological and cardiac functions.[5] Native GLP-1 has a very short circulation time *in vivo* (2-3 min) due to rapid degradation. The dominant metabolizing protease is dipeptidyl peptidase IV (DPP-IV), which inactivates GLP-1 by cleaving two residues from its N-terminus.[6]

Two strategies to activate GLP-1R *in vivo* have been to administer injectable GLP-1 analogues with longer half-lives, and to use DPP-IV inhibitors that decrease metabolism of endogenous GLP-1 and thereby increase its plasma concentration.[7] Injectable GLP-1R agonists include exenatide (Byetta™), a 39-residue peptide with DPP-IV resistance, and liraglutide (Victoza™), a lipidated GLP-1 analogue with greater albumin binding that lowers plasma clearance.[7a] Injectable GLP-1R peptide agonists along with sodium-glucose linked transporter 2

(SGLT2) inhibitors are the only classes of glucose-lowering agents that reduce body weight.[8] Most efforts are currently directed at optimizing GLP-1R peptide agonists to extend half-life, promote greater weight loss and improve tolerability.[9] Additionally, potent non-peptidic GLP-1R agonists are highly sought after, yet only a few weakly potent small molecule allosteric agonists have been reported to date.[9-10]

Agonist activation is thought to involve a 2-site model, with high affinity binding by the C-terminal helical region of GLP-1 (**Figure 1**) to the extracellular N-terminal domain of GLP-1R. This anchors GLP-1 to the receptor[11] and brings its low affinity effector N-terminus (**Figure 1**) into close proximity to an unknown binding site on the receptor. An NMR-derived solution structure of GLP-1 has been reported,[12] as has a crystal structure of GLP-1 bound to the extracellular domain (ECD) of GLP-1R.[13] Key findings were an α-helix in GLP-1 between Thr13-Val33, with a helix break or kink at Gly22,[12-13] and flexible N-terminal region His7-Thr13 with no well defined structure. We planned to use different constraints in the N- and C-termini to investigate what structural features might be important for specific intracellular signaling responses mediated by GLP-1R and associate these to the mechanism of agonist binding. These studies would be enabled with a homology model of GLP-1R based on the recent crystal structure for the related glucagon receptor.[14] Previous studies have used helix-inducing constraints to increase cAMP activity and protease stability of GLP-1, but they reduced receptor affinity.[15-16] Our approach was to first examine GLP-1 bound to our GLP-1R homology model and use molecular dynamics simulations to predict the bound conformation of the N-terminus of GLP-1. These conformations would then be used to design conformational constraints of individual regions of GLP-1 using simple sidechain-to-sidechain or sidechain-to-mainchain lactam constraints. The resulting effects of peptide structure were determined by measuring

GLP-1R affinity, cAMP stimulation and β-arrestin 2 recruitment. Both functional measures have been linked to insulin release.[11] β-arrestin 2, like β-arrestin 1, has a key role in GPCR desensitization, internalization and downregulation,[17-18] and β-arrestins mediate inactivation and subcellular localization of signaling cascades.[19] The structural components of GLP-1 important for β-arrestin signaling or insulin secretion have not been examined previously. A holistic understanding of how the GLP-1 structure and sequence influence GLP-1R binding, intracellular signaling, and insulin release may lead to more effective and safer modulation of GLP-1R for the treatment for type 2 diabetes.

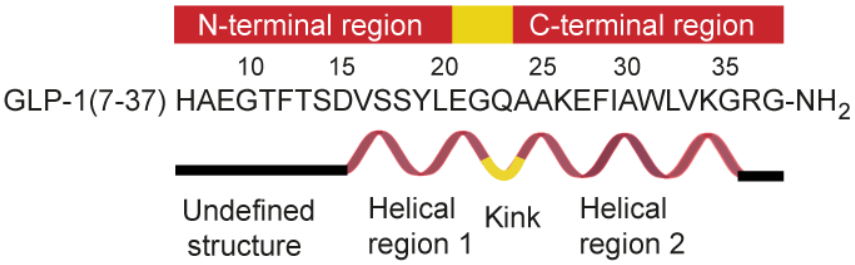

Figure 1. Sequence of GLP-1(7-37)-NH_2 comprising an N-terminal region His7-Asp15 (black string) that is of undefined or random structure and the C-terminal region Val16-Gly35 (red) that is an α-helix, distorted by a kink at Glu21-Gln23 (orange).

RESULTS AND DISCUSSION

Molecular Modeling. To predict receptor-bound conformations of GLP-1 and aid design of constrained GLP-1 analogues, a hybrid homology model for GLP-1R was constructed (Experimental Methods) by aligning the TM region with the high-resolution crystal structure (PDB code: 4L6R) of the related glucagon receptor[14] (**Figures S4, S5**) and by using the crystal structure of the extracellular domain of GLP-1R (PDB code: 3IOL). The six N-terminal residues (H7-AEGT-F12) of GLP-1 were missing in the latter crystal structure, so these residues were modeled into their putative position in the TM bundle of GLP-1R. A 20 ns molecular dynamics simulation sampled possible interactions in this receptor-ligand complex, suggesting that GLP-1 residues from Asp15 to the C-terminus adopted a stable helical structure (**Figure 2A-C**), whereas the N-terminus (His7-Thr13) of GLP-1 adopted a flexible loop (e.g. β-turn at Glu9-Gly10-Thr11-Phe12) (**Figure 2D**) that contacted the receptor TM region (**Figure 2D**). The simulations support previous studies[12a,12b,12d] suggesting that the GLP-1 N-terminus does not fold into a stable α-helix like the C-terminus. A direct interaction between Asp15 in GLP-1 and Arg380 in the receptor has recently been suggested.[20] Our model also captured this electrostatic interaction (**Figure 2D**). Glu9 was also observed in the model to make a hydrogen bond with Arg380, whereas the N-terminus of His7 was hydrogen bonded to Glu387 located in a deeper region of TM6. To gain support for these modeled interactions, we applied *in silico* alanine scanning to residues at the N-terminus of GLP-1. The contribution of the residues to receptor binding was reflected by calculated Δaffinity (kcal/mol), a higher positive value indicating a greater contribution. Encouragingly, the computational alanine scan was in agreement with reported experimental alanine scanning.[8a,8b] Asp15 and His7 were predicted to be the two most important GLP-1 residues for receptor binding, and they were previously shown to be key residues for

GLP-1R activation via Ala mutagenesis. The locations of other N-terminal residues are more uncertain due to the flexibility typical of peptides and GPCRs.[21] We next investigated whether the N-terminus of GLP-1 folded into a turn by determining an NMR structure of a truncated analogue of GLP-1.

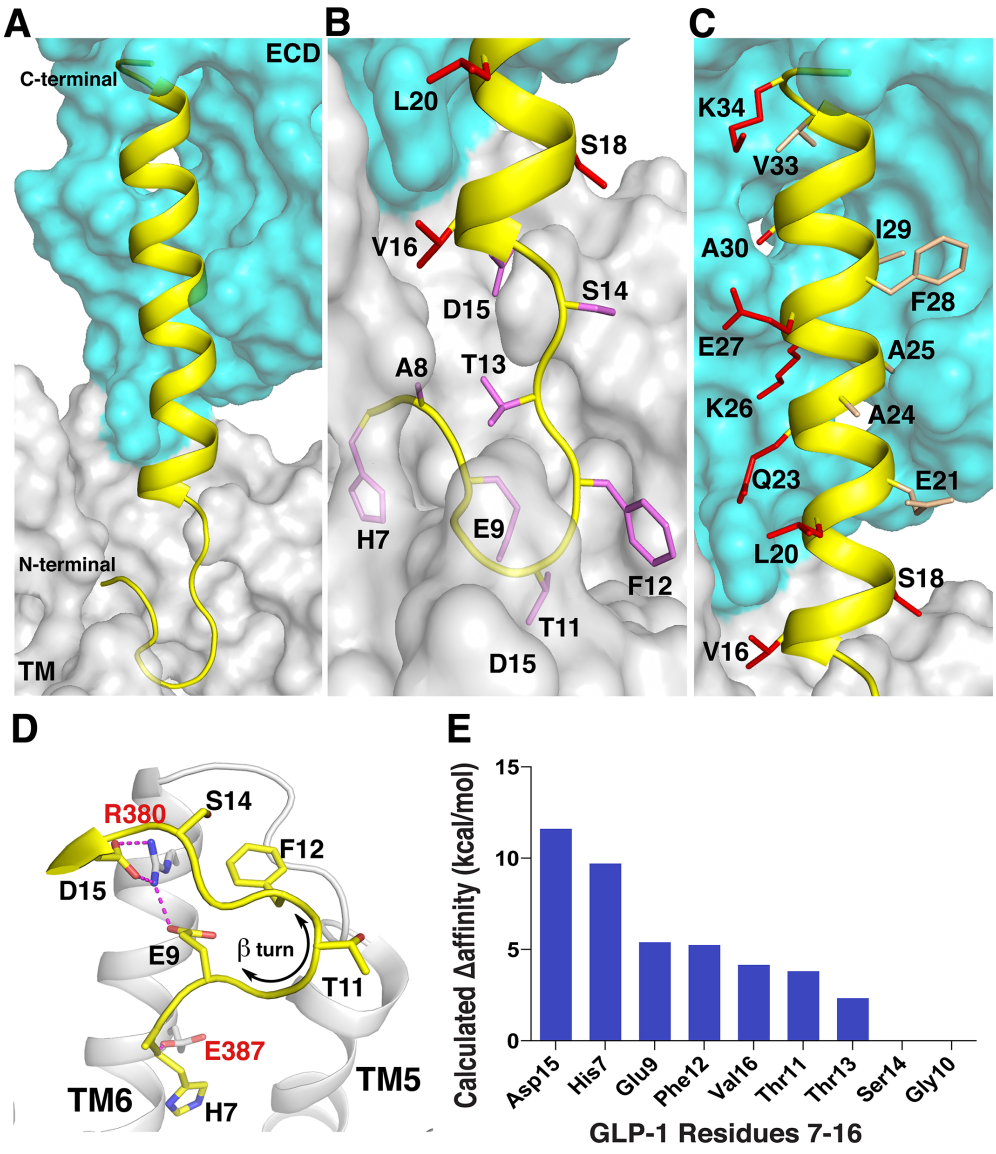

Figure 2: Predicted binding mode of GLP-1 in GLP-1R. (**A**) Overall binding mode of GLP-1 (yellow) in receptor (TM bundle, white; extracellular domain ECD, cyan) sampled at 10 ns of MD simulations. (**B**): TM-ECD interface showing binding of GLP-1 (yellow) with its N-

terminal loop His7-Asp15 sidechains (purple) and C-terminal alpha-helix sidechains (red). (**C**): C-terminal helix (Val16-Lys34) of GLP-1 showing residue side chains (red) exposed to solvent, and considered to be favorable for modification, as well as residue side-chains (wheat) that likely interact with ECD of GLP-1R. (**D**) Model of GLP-1 N-terminus (yellow) bound in TM region of GLP-1R (gray). Residues Glu9 to Phe12 predicted to adopt a β-turn. (**E**) *In silico* alanine scan predicts GLP-1 residues most important for binding to TM region of receptor.

N-terminal structure of GLP-1(7-17). To identify the preferred structure of the N-terminus of GLP-1 in water, we simplified it by replacing C-terminal residues 18-37 with a simple α-helical cyclic pentapeptide, a known helix-nucleating module.[22] Thus, cyclo-(18,22)-HAEGTFTSDVS[**K**YLE**D**]-NH_2 was synthesized, with Lys and Asp (bold) instead of Ser18 and Gly22 in native GLP-1, linked through sidechain-to-sidechain K18-D22 lactam formation. The NMR-derived solution structure of this 16-residue peptide in H_2O/D_2O (9:1) (**Figure 3**) showed an α-helix only between Val16 and Asp22, with a β-turn between Glu9 and Phe12. This was not too surprising as the GTFTSDVS sequence is not predicted to be helix-favoring (rather strand and turn favoring). The cyclic pentapeptide motif was thus incapable of inducing helicity into the eleven N-terminal residues. This result supports the idea that the N-terminus of GLP-1 is independent of the C-terminal helical structure of GLP-1, and that even in this 16-residue fragment a β-turn motif is favored in the Glu9-Gly10-Thr11-Phe12 region (**Figure 3**), as predicted for full length GLP-1 from modeling studies (**Figure 2C**). The importance of a β-turn has also been inferred in other agonists derivatized from the N-terminal nine residues of GLP-1.[23]

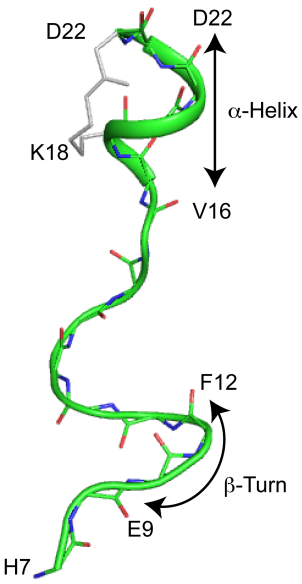

Figure 3. NMR calculated solution structure for GLP-1 analogue cyclo-(18,22)-HAEGTFTSDVS[**K**YLE**D**]-NH_2 in H_2O/D_2O (9:1) at 298K showing two α-helix turns (Val16 to Asp22), stabilized by the lactam bridge (Lys18-Asp22, grey), and a β-turn (Glu9 to Phe12) promoted by the Gly10-Thr11 motif. Only the averaged lowest energy structure is shown.

N-terminal Constraints. Based on the modeling predictions and the NMR structure in water suggesting a turn-favoring motif in the N-terminus of GLP-1, we sought to incorporate different cyclization constraints into the N-terminus of GLP-1(7-37)-NH_2 (compounds **1-8**, **Table 1**) that would induce various turn and helical conformations (vide infra) to test the predictions. The N-terminal amine of His7 was first covalently linked to a side chain of an amino acid at either position 9 (Glu or Cys), position 10 (Glu) or position 11 (Glu or Cys), in attempts to promote different turn conformations (compounds **1**–**5**). A second strategy involved inserting a Lys(i) to Glu(i+n) side chain to side chain lactam constraint between positions 8 (Lys) and either 11 (Glu), 12 (Glu) or 13 (Glu) to form a looser helical region in the N-terminus (compounds **6**–**8**). All of these constrained analogues (**1**–**8**) had much less affinity for GLP-1R and much lower cAMP stimulation or β-arrestin 2 signaling in CHO-GLP-1R cells compared to GLP-1(7-37)-NH_2 (Table 1). This dramatic loss of affinity and activity resulting from modifying the N-terminus of GLP-1 suggested that the structures stabilized by these specific turn constraints were not favorable for binding and/or activation of the receptor.

As a result we investigated the likely structures adopted by these N-terminal cyclic fragments of the GLP-1 analogues using molecular modeling techniques. Since peptide docking and conformational searching can be difficult for long flexible peptides, we first docked a short peptide sequence (HAEGTF-CO_2H) corresponding to the N-terminus of GLP-1 into the TM cavity of the homology model of GLP-1R (**Figure 4**, bottom left and **Figure S6**). Upon docking, this peptide adopted a loop with a turn-like moiety, similar to that observed for full length GLP-1 (**Figure 2D**). Specifically, the peptide docked into a putative binding site surrounded by residues Tyr148, Tyr152, Val194, Arg190, Gln234, Phe367, Glu387, Arg380 (**Figure S6**). It was notable that His7 of the peptide inserted deeply into the TM, sitting above Arg190. However, this ligand docking into the rigid receptor structure resulted in His7 moving away from Glu387, which was different from MD simulations that supported a possible contact between His7 and Glu387. Glu9 of the peptide faced towards Arg380, suggesting an alternative possible salt-bridge interaction, consistent with the above MD simulations of GLP-1 in the receptor that also suggested a direct contact between Arg380 and Glu9 (**Figure 2D**). Of the GLP-1 analogues tested (**1**-**8**), the cyclic constraint in **3** was expected to induce an alpha turn II-aLU,[24a] whilst compounds **6** and **7** with (i, i+3) and (i, i+4) bridges were expected to produce 3_{10}- or α- helical structures[24b,22] and compound **8** with an (i,i+5) may favor the unusual pi-helix.[24c] Compounds **1**, **2** and **4** were subjected to MD simulations to predict their putative structures (**Figure 4**). The distances between the Cα of the first residue *i* to that of the *i+2* in peptides **1**, **2**, and *i+3* Cα atom of peptide **4** (**Figure 4D-F**); the *phi* and *psi* torsional angle of residue Ala8 (*i+1*) in peptide **1**, **2**, and **4**, (**Figure 4H-J**) and of Glu9 and Gly10 in peptide **4** (**Figure 4K,I**), were measured. The average *phi* (-120^o) and *psi* (60^o) torsional angle of Ala8 from peptide **1** suggested that this peptide had an inverse γ-turn at its N-terminus. Peptide **2** was predicted to adopt both β and γ turn conformations based on the

simulations. Peptide **4** was predicted to adopt a distorted beta turn type II between Glu9 to Gly10.

When the conformations of N-terminal constrained cyclic peptides in **1**, **2** and **4** were superimposed (**Figure S7**) on the GLP-1R docked conformation of hexapeptide HAEGTF-CO_2H at two different MD simulation time points (10 ns, 100 ns), it was found that the introduced cyclic constraints maintained the structures of these fragments in a similar fashion to the docked hexapeptide. Unexpectedly, none of these GLP-1 analogues with N-terminal cyclic constraints showed improved cAMP or beta arrestin 2 activities over GLP-1. This may in part reflect the importance for receptor activation of an interaction between His7 of GLP-1 and Glu387 in TM6 of GLP-1R. The discordance in the distance between His7 and Glu387 for the docked hexapeptide versus that in all the docked cyclic constrained analogues may account for the loss of activity. As mentioned above (Figure 2D), Glu9 of GLP1 was predicted to form a salt bridge with Arg380 in the receptor. Introducing cyclization constraints removed the free carboxylic acid of Glu9 in the peptides and this may have directly impacted on the loss of a charge-charge interaction between ligand and receptor for peptides **1** and **2**. While we have not successfully matched the N-terminal GLP-1 conformation that is favored for receptor activation, the results eliminate some possible ways of constraining the N-terminus of GLP-1 and support further studies aimed at stabilizing alternative conformations to realize potent receptor activation. The lack of activity resulting from modifications here of the N-terminus of GLP-1 led us to refocus in this study on inserting structural constraints into the helical C-terminal region of GLP-1.

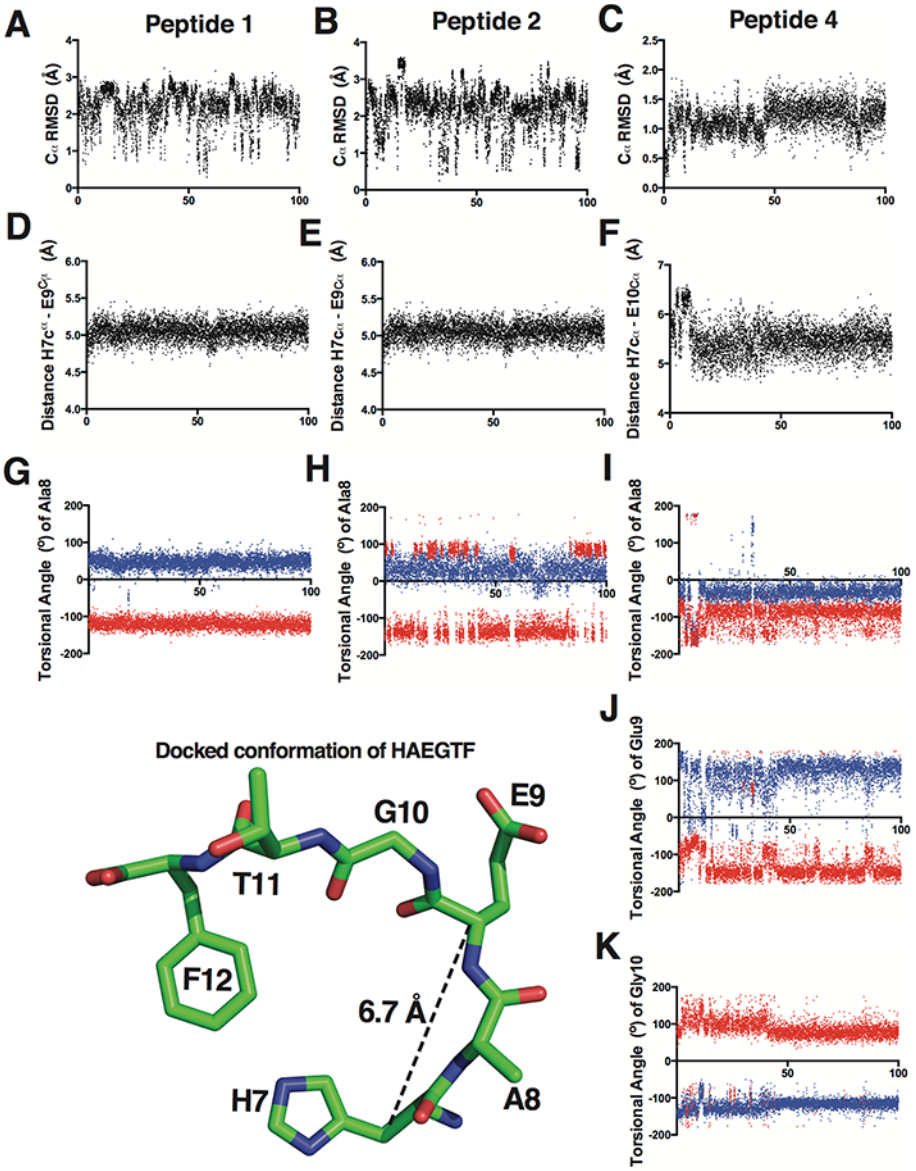

Figure 4: MD simulations of first six N-terminal residues of **1**, **2**, and **4**. (**A**-**C**): Average RMSD variation in all six Cα atoms of cyclic peptides **1**, **2** or **4** from 0-100 ns of the MD simulations. (**D-F**): Distance between Cα of H7 and E9 (**1** and **2)** or E10 (**4**). (**G-K**) Torsional angles (*Phi, red; Psi , blue*) for Ala8 (**1**,**2** and **3**), Glu9 (**3**) and Gly10 (**3**). Bottom left: Docking simulated conformation of hexapeptide HAEGTF corresponding to the N-terminus of GLP-1.

Table 1. Binding affinity (K_i) and receptor activation (EC_{50} cAMP; EC_{50} β-arrestin 2) for N-terminal constrained GLP-1(7-37)-NH_2 analogues **1**-**8**.

#	Peptide[a]	K_i (nM) ± SEM	*N*	cAMP EC_{50} (nM) ± SEM	*N*	β-arrestin 2 EC_{50} (nM) ± SEM	*N*
1	c[H7-E9]GLP-1(7-37)-NH_2	>50	3	150 ± 10	4	>10000	2
2*	c[H7-C9]GLP-1(7-37)-NH_2	--	--	300 ± 30	3	>10000	2
3	c[H7-E10]GLP-1(7-37)-NH_2	34 ± 4	2	>10000	3	>10000	3
4	c[H7-E11]GLP-1(7-37)-NH_2	>50	2	>10000	3	>10000	3
5*	c[H7-C11]GLP-1(7-37)-NH_2	>50	3	>10000	3	>10000	2
6	c[K8-E11]GLP-1(7-37)-NH_2	>50	2	>10000	3	>10000	3
7	c[K8-E12]GLP-1(7-37)-NH_2	>50	4	700 ± 130	3	>10000	3
8	c[K8-E13]GLP-1(7-37)-NH_2	>50	3	>10000	3	>10000	3
	GLP-1(7-37)-NH_2	0.32 ± 0.03	6	0.06 ± 0.01	15	3.7 ± 0.7	4

[a]cyclic peptide region is denoted by c[]. * See Fig S1 for chemical structures of **2** and **5.**

C-terminal lactam bridge constraints. Lactam bridged constraints have previously been incorporated into GLP-1(7-37)-NH_2 and GLP-1(7-36)-NH_2.[4, 15-16] Crosslinking Glu(i) to Lys(i + 4) at positions 18-22, 22-26 and 23-27 slightly reduced binding affinity and without altering cAMP activity. Crosslinking Lys(i) to Glu(i + 4) at positions 16-20, 18-22, 23-27 and 30-34 were well tolerated with slight reductions in binding affinity but equal or better receptor activation, while double and triple Glu(i) to Lys(i + 4) crosslinks at positions 16-20, 18-22, 22-26 and 30-34 gave potent GLP-1 agonists and higher stability to cleavage by DPP-IV and NEP 24.11. Optimal bridge positions from these studies are supported by the crystal structure of GLP-1 bound to the ECD of GLP-1R (**Figure 2C**), in that residues 16, 18, 20, 23, 26, 27, 30, 33 and 34 are solvent exposed and amenable to modification.

We chose to modify GLP-1(7-37)-NH_2 at different positions with a Lys(i)-Asp(i+4) side chain-to-side chain lactam constraint (**Table 2** and **Figure S1**), which induces greater α-helicity for model peptides in water than other similar constraints.[22] Inserting a single helix-inducing constraint at Lys13-Asp17 (**9**) or Lys14-Asp18 (**10**) dramatically reduced receptor binding and cAMP activity, whilst β-arrestin 2 activity was abolished. Repositioning the lactam bridge further towards the C-terminus at Lys16-Asp20 (**11**), Lys18-Asp22 (**12**), Lys18-Glu22 (**13**) or Glu18-Lys22 (**14**) gave compounds with sub-nanomolar binding affinity and potent cAMP and β-arrestin 2 activity. Placing it at Lys30-Asp34 (**15**) slightly reduced binding affinity and β-arrestin 2 activity, but maintained cAMP agonist potency. Thus, a single lactam bridge is well tolerated between residues 16-34, consistent with α–helicity in the homology model (**Figure 2C**). Direct comparison of compound **12** with the previously described[16] **13** and **14** indicates here that all three lactam bridges (Lys-Glu, Glu-Lys, Lys-Asp) were similarly effective in promoting receptor binding and cAMP stimulation, although **13** had lower helicity (30%) than **12** and **14** (42% and 46%, respectively). Incorporating two Lys(i)-Asp(i+4) bridges at 16-20 and 30-34 (**16**) slightly reduced binding affinity and β-arrestin 2 recruitment, but cAMP potency improved (EC_{50} 21pM). Two Lys(i)-Asp(i+4) bridges at 18-22 and 30-34 (**18**) maintained sub-nanomolar binding affinity and improved cAMP activity (EC_{50} 12 pM) compared to GLP-1(7-37)-NH_2 (EC_{50} 60 pM). This increased cAMP potency corresponded to an increase in helicity from 37% to 47%. Together these results indicate that helix-constrained analogues of GLP-1(7-37)-NH_2 with lactam constraints at positions 16–20, 18–22 and/or 30–34 did not greatly impair binding affinity (K_i <1 nM) for GLP-1R. Agonist-induced cAMP activation was improved for **16** (3-fold) and **18** (5 fold). For all compounds, β-arrestin 2 recruitment potency was below 10 nM. These findings

support and complement previous reports[4,15-16] on effects of lactam constraints on receptor affinity and cAMP activity for GLP-1(7-36)-NH_2 analogues.

Table 2. Binding affinity (K_i) and receptor activation (EC_{50} cAMP; EC_{50} β-arrestin 2) for helix constrained GLP-1(7-37)-NH_2 analogues **9**-**18**.

#	Peptide[a]	K_i (nM) ± SEM	*N*	cAMP EC_{50} (nM) ± SEM	*N*	β-arrestin2 EC_{50} (nM) SEM	*N*	% Helicity
	GLP-1(7-37)NH_2	0.32 ± 0.03	6	0.06 ± 0.01	15	3.7 ± 0.7	4	21
9	c[K13-D17]GLP-1(7-37)-NH_2	16 ± 23	4	18.2 ± 7.6	4	>10000	3	36
10	c[K14-D18]GLP-1(7-37)-NH_2	10 ± 4	4	15.3 ± 9.2	3	>10000	3	34
11	c[K16-D20]GLP-1(7-37)-NH_2	0.52 ± 0.19	3	0.054 ± 0.020	3	3.4 ± 1.9	2	36
12	c[K18-D22]GLP-1(7-37)-NH_2	0.35 ± 0.20	3	0.050 ± 0.017	3	4.5 ± 1.4	4	42
13	c[K18-E22]GLP-1(7-37)-NH_2	0.84 ± 0.18	2	0.041± 0.009	3	6.6 ± 0.9	3	30
14	c[E18-K22]GLP-1(7-37)-NH_2	0.80 ± 0.14	2	0.041 ± 0.008	3	8.6 ± 0.5	3	46
15	c[K30-D34]GLP-1(7-37)-NH_2	1.1 ± 0.5	2	0.074 ± 0.022	3	9.2 ± 0.7	3	26
16	c[K16-D20,K30-D34]GLP-1(7-37)-NH_2	1.4 ± 0.9	2	0.021 ± 0.013	3	12 ± 1	3	37
17	c[K18-E22,K30-E34]GLP-1(7-37)-NH_2	--	-	0.050 ± 0.012	3	--	-	17
18	c[K18-D22,K30-D34]GLP-1(7-37)-NH_2	0.94 ± 0.13	2	0.013 ± 0.004	3	6.7 ± 0.4	3	47

[a]cyclic peptide region or regions is denoted by c[].

Mutations to enhance C-terminal helicity. The finding of optimal helix-inducing crosslinks at positions 16-20, 18-22 and 30-34 is consistent with the crystal structure[14] of the C-terminal helical region of GLP-1(7-37)-OH bound to the extracellular domain (ECD) of GLP-1R and with our homology model of GLP-1R bound to GLP-1(7-37)-NH_2 (**Figure 2D**). These showed that Val16, Ser18, Leu20, Gly22, Ala30 and Lys34 are all solvent-exposed and suitable for accommodating crosslinks. A helix-disrupting kink at Gly22 in the crystal structure of GLP-

1(7-37)-OH was not present in the crystal structure of the more potent GLP-1 agonist Ex-4(1-39), which instead shows a continuous α-helix.[13] NMR studies also supported a continuous α-helix in solution from Ser8-Asn28 in Ex-4(1-39), stabilized by Glu16 and Glu17 residues forming salt-bridges with Arg20.[25] We hypothesized that Ala22 in Ex-4(1-39) might help stabilize a helix in this region relative to Gly22 in GLP-1 and thereby increase receptor affinity and activation. Comparative CD spectral analysis of GLP-1(7-37)-NH_2, Ex-4(1-39) and its truncated analogue Ex-4(1-30)-NH_2 supports a link between increasing agonist helicity (**Figure S3**) and increasing GLP-1R mediated cAMP activation. Ex-4 has 12 fold greater cAMP activity than GLP-1(7-37)-NH_2 despite only a 3-fold increase in binding affinity and β-arrestin recruitment potency (**Table 1**).

We therefore sought to similarly promote continuous helicity in the C-terminal region of GLP-1(7-37)-NH_2 by making additional amino-acid substitutions that might complement helix induction by the lactam crosslinks in **19, 20, 21** and **22** (**Table 3**). Comparing the replacement of Gly22 with either a turn-favoring Pro (**19**), a β-sheet-favoring Val (**20**), or an α-helix-favoring Ala residue (**22**), in c[Lys30-Asp34]-GLP-1(7-37)-NH_2 indicated that an uninterrupted α-helix is favored for cAMP release. Proline-substituted derivative **19** had comparable helicity to **15**, whilst **21** showed reduced helicity to 18%. Both analogues had reduced receptor affinity and agonist potency, although the impact was more substantial for the Pro21 substitution. The greater impairment with Pro21 can be attributed to different orientation of the N-terminal region induced by the Pro21-Gly22 motif in **19**, a commonly employed β-turn promoter,[26] and may promote a kinked helix in this region. The reduced activity may also be magnified by a larger helix-breaking effect for proline substitution in this position (Pro 21) versus Pro22. Both **20** and **22** had slightly higher helical propensity than the parent peptide c[Lys30-Glu34]GLP-1 (**15**, **Table 2**).

Gly22 has been reported to be important for GLP-1 receptor binding,[8a] although later structure-activity relationships reported [Ala22]GLP-1(7-36)-NH_2 as an equipotent analogue.[8c] These results show that Gly22Val substitution only slightly reduced potency, while the helix-promoting Gly22Ala change caused a 3-fold increase in potency. Incorporating Ala22 in **16** resulted in agonist **23** with higher helicity (f_{helix} ~46 %) and cAMP agonist activity (EC_{50} 5 pM), whereas affinity and β-arrestin activity were not improved versus parent **16** (**Table 3**). This selective improvement in cAMP activity suggests that a continuous α-helix through this region may improve the positioning of key N-terminal residues that are essential for cAMP activation but not so important for receptor affinity or β-arrestin 2 recruitment.

A second approach to promoting helicity was to insert a "helix N-capping motif" into GLP-1(7-37)-NH_2. It has been shown for native ligands of other class B GPCRs that a hydrophobic residue at position 10 can stabilize a receptor-activating ligand conformation by inducing a helix N-capping motif in conjunction with a Phe or Tyr residue at position 6 or 7.[27] A recent study[28] on lactam-constrained analogues of secretin Sec(1-27) that activates a class B GPCR, guided by molecular mechanics simulations, led to development of a potent antagonist with a Tyr10 insert and a Glu16-Lys20 lactam bridge.[28] We similarly used it here in both linear and lactam-constrained GLP-1 analogues (**24-28**, **Table 3**). A helical N-capping tyrosine residue (Tyr16, Tyr17) was incorporated into GLP-1(7-37)-NH_2 (**24, 25**). Tyr16 was also incorporated into **15** and **18** giving compounds **26** and **27** to potentially enhance the effects of lactam bridges Lys18-Asp22 and Lys30-Asp34. The tyrosine substituent at position 16 of **24** improved both binding affinity and cAMP activity by approximately 2-fold compared to GLP-1(7-37)-NH_2, whereas Tyr substitution at position 17 attenuated both binding affinity and activity. The Tyr16 substituent in lactam-constrained **26** and **27** gave high cAMP activity (EC_{50} 33 pM and 15 pM, respectively)

and binding affinity (K_i < 1 nM), whilst β-arrestin 2 activity was maintained (EC_{50} < 10 nM) versus the parent peptides. The Ala22 mutant of **26**, compound **28**, had increased helicity (40%) and a 3 fold increase in cAMP activity (EC_{50} 11 pM) whilst binding affinity and β-arrestin 2 activity were similar to the parent. These results indicate that introducing Tyr16 into GLP-1 (7-37)-NH_2 and **15** to give **24** and **26** enhanced binding affinity, cAMP activity and β-arrestin 2 recruitment by approximately 2-fold. This improvement was not observed when Tyr16 was introduced into double lactam-bridged compound **27**. Introduction of Ala22 into **26** to give **28** resulted in a 3-fold improvement in cAMP potency, similar to the increase observed for A22 in compound **22**. The influence of helicity on activities of the highly potent GLP-1R agonist Exendin-4(1-39)NH_2 (HGEGTFTSDLSKQMEEAVRLFIEWLKNGGPSSGAPPPS-NH_2) and its truncated analogue, Exendin-4 (1-30)-NH_2 (HGEGTFTSDLSKQMEEAVRLFIEWLKNGG-NH_2)**,** was also investigated. CD spectroscopy demonstrated that residues 31-39 were important for helicity. Ex-4(1-39)NH_2 (76% helicity) with greater helicity than Ex-4(1-30)NH_2, consistent with the tryptophan cage motif at the C-terminus of Ex-4 inducing helicity throughout the structure. This greater helicity corresponded to increased binding affinity and higher cAMP and β-arrestin 2 potencies for Ex-4(1-39) over Ex-4(1-30).

Table 3. Binding affinity (K_i) and receptor activation (EC_{50} cAMP; EC_{50} β-arrestin 2) for GLP-1(7-37)-NH_2 analogues **19**-**28** versus Ex-4(1-30)NH_2 and Ex-4(1-39)NH_2.

#	Peptide[a]	K_i (nM) ± SEM	*N*	cAMP EC_{50} (nM) ± SEM[b]	*N*	β-arrestin 2 EC_{50} (nM) ± SEM	*N*	% Helicity
19	c[K30-D34][P22]GLP-1(7-37)-NH_2	18 ± 2	2	0.35 ± 0.16	3	33 ± 2	3	26
20	c[K30-D34][V22]GLP-1(7-37)-NH_2	1.5 ± 0.3	2	0.10 ± 0.05	3	9.0 ± 1.6	3	29
21	c[K30-D34][P21]GLP-1(7-37)-NH_2	>50	2	20 ± 9	3	>1000	2	18
22	c[K30-D34][A22]GLP-1(7-37)-NH_2	1.7 ± 0.4	2	0.020 ± 0.006	3	11 ± 1	3	29
23	c[K16-D20,K30-D34][A22]GLP-1(7-37)-NH_2	1.4 ± 0.1	2	0.004 ±0.001	3	11 ± 3	3	46
24	[Y16]GLP-1(7-37)-NH_2	0.23 ± 0.1	4	0.035 ± 0.003	3	1.5 ± 0.8	3	15
25	[Y17]GLP-1(7-37)-NH_2	26 ± 5	3	1.9 ± 0.3	3	58 ± 10	3	-
26	c[K30-D34][Y16]GLP-1(7-37)-NH_2	0.49 ± 0.17	2	0.023 ± 0.003	3	3.4 ± 0.3	3	29
27	c[K18-D22,K30-D34][Y16]GLP-1(7-37)-NH_2	0.82 ± 0.40	2	0.009 ± 0.003	3	8.8 ± 1.6	3	49
28	c[K30-D34][Y16][A22]GLP-1(7-37)-NH_2	0.47 ± 0.12	2	0.011 ± 0.004	3	4.6 ± 0.4	3	40
	Ex-4(1-30)-NH_2	0.49±0.08	3	0.025 ± 0.009	3	2.9 ± 0.2	4	49
	Ex-4(1-39)-NH_2	0.11 ± 0.02	4	0.006 ± 0.001	3	1.0 ± 1.0	6	76

[a] cyclic peptide region is denoted by c[].[b] See figure SX for representative cAMP activation curves

Relationship between helicity and receptor binding/signaling. The relationship between helicity and cAMP stimulation (**Figure 5A**) or binding affinity (**Figure 5B**) or β-arrestin-2 recruitment (**Figure 5C**) is shown for each of the lactam-bridged helix-constrained peptides **11**, **12**, **15**, **16**, **18**, **20**, **22**, **23**, **26**, **27**, **28** versus GLP-1, Ex-4(1-30) and Ex-4(1-39). The Ex-4 analogues were chosen for their greater α–helicity than GLP-1(7-37)-NH_2 and comparable or better binding affinities.

Figure 5 plots compounds in order of increasing cAMP activity (left vertical axis, blue) from left to right against helicity (right vertical axis, white) (**Figure 5A**) and reveals the strongest correlation (R= 0.77). Compounds with increased α–helicity, except **15** and **20**, had greater cAMP activity than the parent GLP-1(7-37)-NH_2. Of compounds with helicity greater then 40%, only **12** did not have activity below 30 pM. Compound **11** also deviates from this trend with helicity 36% and cAMP 54 pM. This data suggests that a single KD lactam bridge in these positions does not stabilize the peptide sufficiently to increase cAMP activity. The cAMP potencies of the lactam bridge-containing compounds (**18, 23, 27, 28**) and the highly helical compounds (EX-4(1-30)-NH_2, EX-4(1-39)-NH_2) were the most potent. Thus, there was an apparent relationship between α–helicity and cAMP potency. On the other hand, plotting the same series of compounds against binding affinity (**Figure 5B**) and β-arrestin-2 recruitment (**Figure 5C**) showed poor correlations with helicity (R = 0.26, 0.30, respectively).

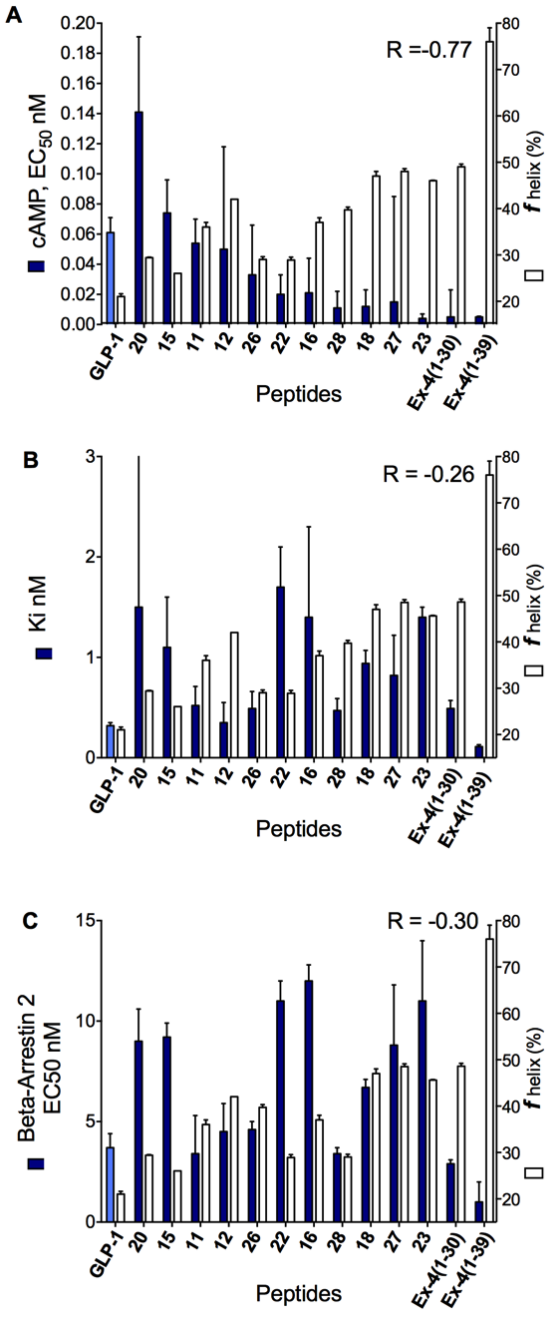

Figure 5. Relationship between helicity and (**A**) cAMP activity or (**B**) binding affinity or (**C**) β-arrestin-2 recruitment.

The positive correlation between α–helicity and cAMP signaling, but not binding affinity or β-arrestin 2 recruitment, suggests that the orientation of peptide side-chains in the middle and C-terminal end of GLP-1 modulate a receptor conformation important for Gs coupling. Alanine scans of GLP-1 have identified His7, Gly10, Phe12, Thr13, Asp15, Tyr19, Glu21, Phe28 and Ile29 as the most important residues for binding affinity and cAMP.[11] Asp15, Tyr19, Glu21, Phe28 and Ile29 are within the region where lactam constraints were introduced in this study. Thus structural stabilization of the orientation of these residues may have increased cAMP activation. If helix induction does not affect structure between residues 7-15, as observed in **Figure 2** and predicted in **Figure 1C**, then it is unlikely that helicity in the C-terminal half will affect N-terminal affinity or activation. However, helicity may have an impact on the orientation of the N-terminus, so further work is needed to better understand the structure of the N-terminal region of GLP-1 and how this has an impact on receptor activation. β-arrestin 2 was not greatly affected by increasing helicity (**Figure 5B**), suggesting that the most important residues for β-arrestin 2 activation are not located in the α–helical C-terminal half of GLP-1. However, making changes in this region that impacts binding affinity may also affect β-arrestin 2 since these were highly correlated (**Figure 6B**).

Relationship between receptor binding and signaling. The relationships between GLP-1R binding affinity, cAMP release, and β-arrestin 2 recruitment for compounds **11–28** are summarized in **Figure 6**. Compounds **1–10** were excluded from these plots because β-arrestin 2 recruitment was not detected at the highest concentration tested (Table 1). Overall, high binding affinity led to potent activation of both cAMP and β-arrestin 2 signaling pathways. However, the binding affinity correlated more poorly (Spearman correlation coefficient, r_s) with cAMP activity (**Figure 6A**) than with β-arrestin 2 activity (**Figure 6B**).

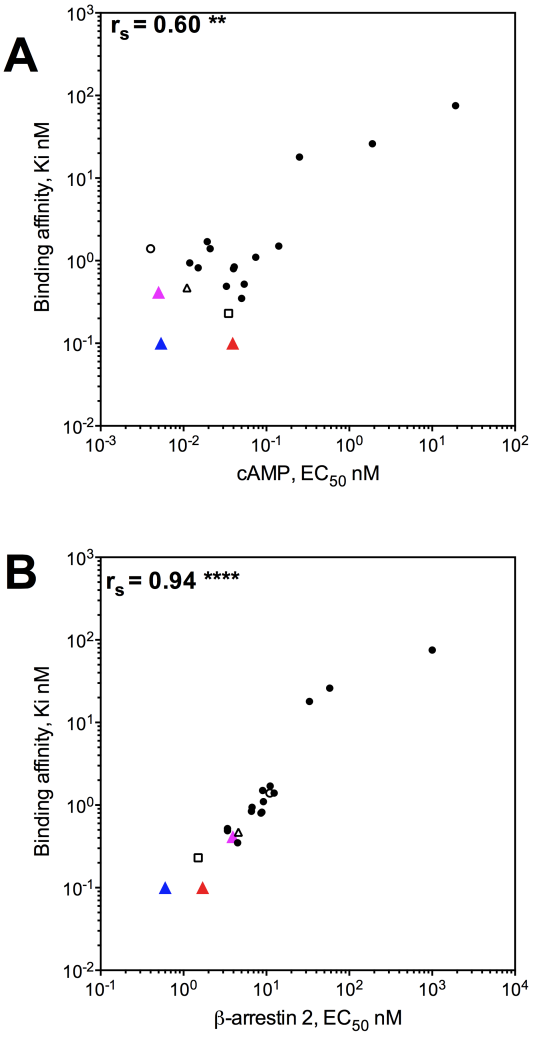

Figure 6. Relationships for constrained GLP-1 analogues **11–28** (n=20) between **(A):** GLP-1R binding affinity and cAMP stimulation; and (**B**) GLP-1R binding affinity and β-arrestin 2 signaling; and (GLP-1 (7-37)-NH_2, red; Ex4(1-30)NH_2, pink; Ex4(1-39), blue. Spearman correlation coefficient r_s (two-tailed p-value < 0.05 * and < 0.0001 ****). O = **23**, □ = **24**, Δ = **28**.

Insulin release. Both cAMP[5] and β-arrestin 2[29,30] signaling have been associated with GLP-1 induced insulin secretion from pancreatic β-cells. Twelve peptides (GLP-1, Ex4(1-39), Ex4(1-30), **10, 16, 19, 20, 21, 23, 25, 27** and **28**) were examined for their ability to potentiate glucose-stimulated insulin release from INS-1 cells (**Figure 7A)**. The highly α-helical (46%) **23** had the most potent cAMP activity (EC_{50} 5 pM) and was equipotent to Exendin 9-39 in inducing insulin release (EC_{50} 0.25 nM). These compounds were more potent then GLP-1(7-37)-NH_2 and Ex-4(1-30)-NH_2 (EC_{50} 0.9 nM). Plotting insulin release potencies against cAMP activity (**Figure 7B**) revealed a strong correlation (r_s = 0.95). On the other hand, compounds **25** and **10** had comparable cAMP potencies, very different β-arrestin-2 activities (EC_{50} 58 nM vs $>10^5$ nM), yet both induced insulin release (EC_{50} 16 vs 50 nM). Similarly, while compounds **10** and **21** had no measurable β-arrestin-2 activities, they both bound to GLP-1 (Ki 10 nM), increased cAMP signaling (EC_{50} 1.2 nM and 20 nM, respectively) and were able potentiate insulin release (EC_{50} 50 nM and 130 nM, respectively). These findings are consistent with cAMP activation being sufficient for, and the more important signaling pathway to, insulin release. These results need to be interpreted carefully, since only INS-1 cells were studied, but these conformationally biased ligands could be helpful for interrogating signaling pathways of importance for insulin release in human pancreatic islets.

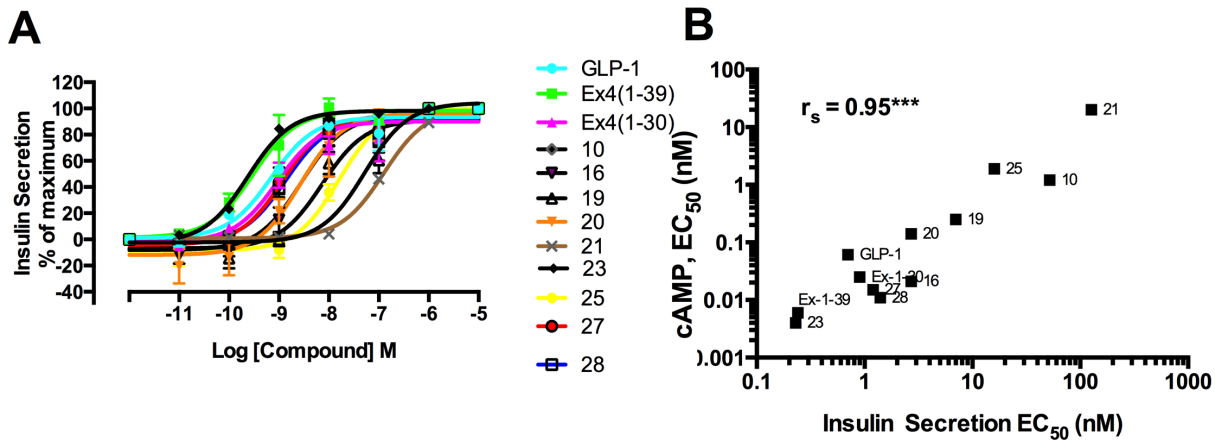

Figure 7. (**A**) Potentiation of glucose-stimulated insulin secretion from INS-1 cells by GLP-1, Ex4(1-39), Ex4(1-30), **10, 16, 19, 20, 21, 23, 25, 27 and 28.** Insulin secretion was normalised to 100% for the maximum response of each compound. (**B**) Correlation of insulin release and cAMP potencies for tested peptides. r_s = Spearman correlation coefficient (two-tailed p-value < 0.05 * , < 0.01**, < 0.001 ***).

CONCLUSION

A combination of receptor-ligand homology modeling and dynamics simulations were used to aid the design of structurally constrained peptide analogues of GLP-1(7-37)-NH_2 for assessment of the effects of structure on receptor binding affinity, cAMP release and β-arresitin-2 recruitment, as well as insulin release from pancreatic cells. Incorporation of Lys(i)-Asp(i+4) lactam constraints into human GLP-1(7-37)-NH_2, coupled with a Gly22Ala(**23**) or Val16Tyr (**27**, **28**) substitution, increased peptide α-helicity in the C-terminus as well as cAMP activity, whilst maintaining but not increasing receptor binding affinity and β-arrestin-2 recruitment. From a range of analogues with cyclic constraints and positional mutations, potent agonists **11**–**13**, **15**, **16**, **18** and highly potent agonists **22**, **23**, **24**, **26**, **27** and **28** were identified as being superior agonists to GLP-1(7-37)-NH_2 in inducing cAMP stimulation. Compounds with greater cAMP activity were more α–helical than GLP-1(7-37)-NH_2. Commonly used linear GLP-1 agonists had activity at low nanomolar concentrations in the β-arrestin 2 recruitment assay, with full length Exendin-4 being the most potent (EC_{50} 1 nM). A stronger correlation was observed between binding affinity and β-arrestin 2 signaling (r_s = 0.94) than with cAMP stimulation (r_s = 0.64). However, it was found here that cAMP stimulation, rather than β-arrestin 2 recruitment, was the better predictor of insulin release from INS1 cells. Further investigations into ways of constraining conformation in the N-terminal region of GLP-1 may lead to even more effective GLP-1R agonists with differential or biased pathway signaling that may or may not stimulate insulin release.

EXPERIMENTAL SECTION

Chemicals and Solvents. See Supporting Information (SI)

Peptide Synthesis. Peptides were synthesized using standard Fmoc solid phase peptide synthesis protocols[22] and lactam bridges were formed as described.[22] Briefly, the chemistry was conducted on Rink amide resin (low loading 0.38 mmol/g; Novabiochem) at a 50 μM scale on a Symphony Multiplex Synthesizer. Amino acids (4 eq.) were activated using HCTU (4 eq.) and DIPEA (8 eq.) in DMF (2 × 10 min) prior to remove N-terminal Fmoc protecting group using 20% piperidine in DMF (2 × 5 min). Formation of lactam constraints required a first selective side-chain deprotection of the phenylisopropyl ester (Opip) on aspartic or glutamic acid and of the methyl trityl (Mtt) group on lysine from the peptide-resin using 3% TFA in DCM (2 × 5 min). Second, cyclization was achieved on peptide-resin with a 6mL solution of PyBOP / DIPEA (1 g/400 μL) in DMF over 10–15 h and under continuous nitrogen bubbling. The procedure was repeated for multiple cyclizations. Peptides were cleaved of the resin using a solution of TFA/TIPS/H_2O (95/2.5/2.5) over 2 h before being filtered through original reaction vessels and washed with DCM (3 times). Solutions were then dried under nitrogen; the resulting materials were precipitated with ice-cold diethyl ether and lyophilized. Crude peptides were dissolved in a solution of H_2O/MeCN, filtered through disposable syringe filter unit (NP045AN, Advantec) before being purified on reverse-phase Schimadzu HPLC system; Phenomenex C18 10 μm, 100 Å, 250 × 21.2 mm semi-preparative column, 20 mL/min, isocratic 20% solvent B (H_2O/MeCN 10/90 with 0.1% TFA modifier) in solvent A (H_2O with 0.1% TFA modifier) over 5min and gradient 20%–70% solvent B in solvent A over 30 min. HPLC traces were monitored by UV detectors at 214 and 254 nm. Peptides were >90% purity by analytical UHPLC-MS method: Schimadzu HPLC system Waters Acquity UPLC HSS T3 column, 1.8 μm, 2.1 mm × 50 mm –

gradient 0-100% solvent B (H_2O/MeCN 10/90 with 0.05% formic acid) in solvent A (H_2O with 0.05% formic acid) over 4 min at 0.4 mL/min coupled to LCMS-2020, single quadrupole liquid chromatograph mass spectrometer (Table **4**).

Table 4. Peptide UPLC-MS characterization.

#	t_R (min)	Mol. Weight (Da)	Isotopic ions m/z $_{obs}$ $[M+nH]^+$ (n)	Purity % UPLC
GLP-1	2.25	3352.7	1678.3 (2), 1119.2 (3), 839.6 (4), 672.1 (5)	>95
Ex-4	1.96	4184.1	1396.5 (3), 1047.7 (4), 838.4 (5)	>95
trEx-4	2.02	3406.7	1136.5 (3), 852.7 (4), 682.3 (5)	>95
1	2.77	3350.7	1675.0 (2), 1118.0 (3), 838.6 (4)	>95
2	2.17	3382.7	1690.5 (2), 1128.6 (3), 846.7 (4)	>95
3	2.78	3422.8	1710.9 (2), 1141.7 (3), 856.6 (4)	>95
4	2.70	3378.7	1688.7 (2), 1127.0 (3), 845.6 (4)	>95
5	2.73	3410.8	1704.6 (2), 1137.7 (3), 853.7 (4)	>95
6	2.62	3421.8	1710.4 (2), 1141.7 (3), 856.4 (4)	>95
7	1.98	3375.7	1688.8 (2), 1126.2 (3), 845.0 (4), 676.2 (5)	>95
8	2.59	3363.7	1681.7 (2), 1122.2 (3), 841.9 (4)	>95
9	2.27	3391.7	1696.9 (2), 1131.6 (3), 849.2 (4), 679.6 (5)	>95
10	2.76	3405.8	1703.8 (2), 1136.3 (3), 852.6 (4), 682.2 (5)	>95
11	1.91	3367.6	1684.8 (2), 1123.6 (3), 842.8 (4), 674.6 (5)	>95

12	2.66	3435.8	1718.8 (2), 1146.2 (3), 860.0 (4), 688.3 (5)	>95
13	2.31	3447.9	1725.9 (2), 1150.9 (3), 863.5 (4), 691.1 (5)	>95
14	2.30	3447.9	1725.9 (2), 1150.9 (3), 863.5 (4), 691.1 (5)	>90
15	2.66	3378.7	1691.3 (2), 1127.9 (3), 846.2 (4)	>90
16	2.18	3391.6	1697.7 (2), 1132.2 (3), 849.4 (4)	>90
17	2.68	3487.7	1745.9 (2), 1164.3 (3), 873.6 (4)	>95
18	2.76	3459.7	1731.8 (2), 1154.9 (3), 866.5 (4)	>95
19	2.67	3418.7	1711.4 (2), 1141.3 (3), 856.2 (4)	>95
20	2.82	3420.7	1712.3 (2), 1141.9 (3), 856.7 (4)	>90
21	2.79	3346.6	1675.3 (2), 1117.2 (3), 838.2 (4)	>95
22	2.68	3392.7	1698.3 (2), 1132.6 (3), 849.7 (4)	>95
23	2.04	3418.7	1710.3 (2), 1140.6 (3), 855.8 (4), 684.9 (5)	>95
24	2.16	3445.8	1722.1 (2), 1149.5 (3), 862.2 (4)	>95
25	2.67	3523.7	1176.1 (3), 882.4 (4), 706.2 (5)	>95
26	2.66	3456.7	1730.3 (2), 1153.9 (3), 865.7 (4)	>95
27	2.51	3442.6	1723.3 (2), 1149.2 (3), 862.2 (4)	>95
28	2.59	3405.6	1704.8 (2), 1136.9 (3), 852.9 (4)	>95

N.d. = not detected

CD measurements: were performed using a Jasco model J-710 spectropolarimeter as previously decribed,[22] full experimental details are described in the SI.

NMR Spectroscopy and Structure Calculations: Full experimental details are provided in the SI.

Homology Model of GLP-1R(29-463). The LALIGN server (http://embnet.vital-it.ch/software/LALIGN_form.html) gives a 49.4% between the glucagon receptor and GLP-1 receptor. The most recently disclosed crystal structure[14] of the glucagon receptor (PDB: 4L6R) was considered an adequate template for homology modelling of the transmembrane region of GLP-1R. The extracellular domain (residues 29-127) of GLP1R was modelled based on the crystal structure of GLP1R (PDB: 3IOL). The sequences of full GLP-1R sequence (GI:565107), GLP-1R extracellular domain (GI:262118665), and glucagon receptor (GI:439690) were retrieved from NCBI protein search panel. Based on the resolved coordinates of the template proteins, residues from 29 to 463 of the GLP-1R were modelled. Sequence alignment consisting of the query and the two templates were first performed in ClustalW version 2[31] and the final alignment was further adjusted in Jalview (version 2.4).[32] Five GLP1R full models were generated using Modeller 9.10.[33] The quality of the models was indicated in both DOPE score and GA341 score within Modeller. The best model was selected based on visual inspection of the structures with the most reasonable location for ECL1. The selected model was submitted to SWISS-MODEL (http://swissmodel.expasy.org) for quality assessment. The PROCHECK statistics-derived Ramachandran plot of the constructed transmembrane model of GLP-1R is illustrated in Figure S3.

Molecular Dynamics (MD) Simulations. The receptor-ligand complex (Figure S4) was first prepared with a standard protocol in "Protein Preparation Wizard" within Maestro, version 9.5 (Schrödinger, LLC, New York, NY, 2013). Hydrogen atoms were added, and hydrogen bond assignment, tautomer, and protonation of amino acids at pH 7.4, were optimized. The prepared structure was then embedded in 1-palmitoyl-2-oleoyl-sn-glycero-3-phosphocholine (POPC) membrane via the membrane set up panel in DesmondMolecular Dynamics System v3.5 (D. E.

Shaw Research, New York, NY, 2013). The SPC model was used to describe water molecules.[34] Neutralization of the system was further implemented by the addition of 5 net Na^+ ions at physiological concentration of 0.15 M. After solvating the whole system, a default membrane protein relaxation protocol generated in Desmond was used for further simulation with Berendsen coupling. The all-atom optimized potential for liquid simulations (OPLS-2005) force field implemented as the default force field in Desmond was adopted for all molecules in the system. Prior to the MD production, two stages of minimization were applied. The first stage included minimization with restraints on solute heavy atoms with a force constant of 50 kcal/mol/$Å^2$. The second stage was the minimization without any restraints. The minimized system was further relaxed before the actual simulation. Six steps were included in this stage: 1) heating up the system to 300K with NVT ensemble with Berendsen coupling for 60 ps. 2) a 200 ps equilibration NPT restrained on heavy atoms. 3) NPT equilibration of solvent and lipids for 100 ps. 4). NPT with protein heavy atoms for 600 ps. 5) NPT equilibration with protein c alpha atoms at 2 kcal/mol. 6) NPT with no restraints for 100 ps. Finally, MD simulation was performed with NPT ensemble at 300K temperature and 1.01325 bar for pressure. Berendsen coupling for both thermostat and barostat was adopted with an integration of 2 fs. Coulombic interactions were calculated using a cutoff radius 9 Å. Long-range electrostatic interactions were calculated with Particle Mesh Ewald (PME) method.

Molecular Dynamic Simulations of Cyclic Peptides. Structures of cyclic peptides (first 6 residues) **1**, **2**, **4** were constructed in Maestro, version 9.5 (Schrödinger, LLC, New York, NY, 2013). The structures were first minimized using the geometry clean up function available in Maestro. Peptides were solvated in TIP3P water box. The solvated system was neutralized by adding Na^+ and Cl^- ions at physiological concentration of 0.15 M. Molecular dynamics

simulations were performed with the same settings as described above. Each simulation was carried out for 100ns.

cAMP Accumulation Assay.[23] Cells were washed with PBS, lifted using Cell Dissociation Solution (SIGMA®), counted, centrifuged (1500 rpm, 5 min), re-suspended in cAMP assay buffer (HBSS, 5.6 mM glucose, 0.1% BSA, 0.5 mM IBMX, 5 mM HEPES, pH 7.4) then plated in ProxiPlate Plus 384-shallow well plates (Perkin Elmer) at a density of 1000 cells per well. Cells were then treated with compounds over a range of concentrations (1 pM to 10 μM) and incubated at room temperature for 30 min. Accumulated cAMP was then assessed using LANCE® *Ultra* cAMP kit (Perkin Elmer). Following manufacturer instructions, cells were lysed using kit lysis buffer followed by the addition of cAMP specific antibody labeled with *Ulight*™ dye, and europium chelate-labeled cAMP tracer to each well then incubated at room temperature for 1 hr. The plate was read using a PHERAstar FS (BMG Labtech) plate reader. For analysis, 665 nm raw signal was normalised as a percentage of GLP-1 665 nm raw signal control on each plate. Details of cell culture and membrane preparation are provided in the supporting information.

GLP-1R Radioligand SPA Binding Assay. Test compounds were assessed for receptor binding affinity in CHO cells transfected with human GLP-1R. Compounds were half log serially diluted in DMSO. Each compound (1 μL) was added to appropriate wells of a 384-well plate (CoStar 3657) in duplicate. These were then diluted in binding buffer (50 mM HEPES pH 7.4 (Gibco Cat # 15630-080), 5 mM $MgCl_2$, 0.01% v/v Pluronic F-127 0.01% v/v (Invitrogen Cat # P-6866), 5% glycerol v/v (Roche Applied Science catalogue no. 03117502001) and 0.2% w/v Fatty Acid Free BSA (Sigma Cat # A6003)), and the compound/binding buffer solution (11 μL) was transferred from each well to a white Matrix ScreenMates 384 Well Assay Microplate

(Matrix Cat # 4322). Unlabeled Exendin-4 (Tocris cat # 1933) at a final concentration of 1 ¦ M, was used to determine non-specific binding. CHO-hGLP-1R membranes were thawed and diluted in binding buffer 0.5 ¦ g/25 ¦ L, and 25 µL were added to each well. WGA coated PVT SPA Beads (Perkin Elmer Cat # RPNQ0060) were diluted in binding buffer to a concentration of 2 ¦ g/µL, and 25 µL was added to each well for a final concentration of 50 ¦ g/well. [^{125}I]-GLP 7-36 (Perkin Elmer Cat # NEX308) was diluted in binding buffer to 850 pM, and 25 µL was added to all wells for a final assay concentration of 250 pM. The plate was incubated for 30 min w/shaking at ~25 °C. The assay plate was then placed in a Wallac Trilux MicroBeta, plate-based scintillation counter for 10 h, after which the radioactivity associated with each well was measured using a normalized protocol at 1 min read/well. The K_d for [^{125}I]-GLP-1 7-36 was determined by carrying out saturation binding, with data analysis by non-linear regression, fit to a one-site hyperbola (Graph Pad Prism). IC_{50} determinations were made from competition curves, analyzed with a proprietary curve fitting program (SIGHTS) and a 4-parameter logistic dose response equation. K_i values were calculated from IC_{50} values, using the Cheng-Prusoff equation.

β-arrestin-2 assay. β-arrestin-2 recruitment was measured using the DiscoveRx PathHunter® enzyme complementation technology. A CHO-K1 GLP1R β-arrestin-2 cell line (DiscoveRx Cat # 93-0300C2, lot 08A1803) was grown according to the manufacturer's protocol. Briefly, CHO hGLP-1 β-arrestin-2 cells were removed from cryopreservation, re-suspended in 40 mL of Dulbecco's Phosphate Buffered Saline (DPBS) and centrifuged at 800 x g. The cell pellet was then re-suspended in 50 mL of assay medium (1x F-12 nutrient mix HAMS (Invitrogen #11765-054), 10% heat inactivated fetal bovine serum (HIFBS; Sigma Cat # F4135-100), 5 mL of 100X Pen-Strep (Gibco Cat #15140-122), 5 mL of 100X L-Glutamine (Gibco Cat # 25030-081) and

800 ug/mL Geneticin (G418) (Invitrogen Cat #10131035)) and 300 ug/mL Hygromycin B (Invitrogen Cat # 10687-010)). Cells were centrifuged at 800 x g and then re-suspended in assay medium. Cells were counted and 5000 cells was added to each well of a white Greiner 384-well plate (Greiner cat # 781098). After an overnight incubation at 37 °C, cells were stimulated with varying concentrations of compounds diluted in growth medium. After a 90 min incubation at 37 °C, 10 µL of Galacton Star β-galactosidase substrate (PathHunter Detection Kit (DiscoveRx Cat # 93-0001) was added to each well. The plates were then incubated at room temperature for 60 min and changes in luminescence were measured with an Envision 2104 multilabel plate reader. EC_{50} determinations were determined using GraphPad Prism (4-parameter logistic dose response equation).

INS-1 cell culture and insulin secretion. Rat INS-1 insulinoma insulin secreting cells were cultured at the University of Queensland at 37 °C, 5% CO_2 in 11 mM glucose RPMI1640 media (gibco®) containing additional 1% Na^+ pyruvate (gibco®), 1% HEPES (1 M, pH 7.4) (gibco®), 1% GlutaMAX™ (gibco®), 1% Pen Strep (gibco®), 10% heat inactivated fetal bovine serum HIFBS and 50 µM β-Mercaptoethanol (SIGMA®). INS-1 cells were washed with PBS, lifted with TrypLE Express (gibco®), counted, centrifuged (1500 rpm, 5 min), re-suspended in 11 mM glucose RPMI 1640 culture medium (described in INS-1 cell culture) and seeded into 96-well tissue culture treated plates at a density of 50,000 cells per well and incubated for 4 days. Prior to treatment with compounds, existing cell media was removed from wells then cells were pre-incubated in 3 mM glucose RPMI1640 media for 1 h. Pre-incubation media was then replaced with fresh 11 mM glucose RPMI1640 media before cells were treated with compounds over a range of concentrations (10 pM to 10 µM) then incubated for 1 h. Supernatant was collected then

tested for insulin content using cisbio HTRF® insulin assay kit (62INSPEB) following manufacturers instructions.

AUTHOR INFORMATION

Corresponding authors: * E: d.fairlie@imb.uq.edu.au, T: +61-733462989 F: +61-733462990; and E: t.hill@imb.uq.edu.au. T: +61-733462987. F: +61-733462990.

Author Contributions. Compounds were designed by DF, FP, TH and AD; synthesized and characterised by FP, TH, and AD; examined for helicity and three dimensional structure using CD and NMR spectra by FP and HH; and evaluated for cAMP and insulin release by JM and AC and for binding affinity and β-arrestin 2 by DRD. WX prepared the GLP-1R homology model and performed GLP-1 docking and MD simulations. DF, FP, TH and DG wrote the manuscript. All authors contributed editorial input and to analysis of the results.

Notes. The authors declare no competing financial interests.

ACKNOWLEDGMENTS

We thank the Australian National Health and Medical Research Council for a Senior Principal Research Fellowship to DF (1027369), the Australian Research Council for grants (LP 110200213, DP130100629) and for a Centre of Excellence in Advanced Molecular Imaging (CE140100011). We also thank the Pfizer Emerging Science fund and the Queensland Government (CIF grant) for support of this work.

REFERENCES

1. Hollenstein, K.; de Graaf, C.; Bortolato, A.; Wang, M.-W.; Marshall, F. H.; Stevens, R. C., Insights into the structure of class B GPCRs. *Trends Pharmacol. Sci.* 2014, *35*, 12-22.

2. Cho, Y. M.; Merchant, C. E.; Kieffer, T. J., Targeting the glucagon receptor family for diabetes and obesity therapy. *Pharmacol. Ther.* 2012, *135*, 247-278.

3. Golay, A.; Ybarra, J., Link between obesity and type 2 diabetes. *B. Prac. Res. Clin. Endo. Metab.* 2005, *19* , 649-663.

4. Miranda, L. P.; Winters, K. A.; Gegg, C. V.; Patel, A.; Aral, J.; Long, J.; Zhang, J.; Diamond, S.; Guido, M.; Stanislaus, S.; Ma, M.; Li, H.; Rose, M. J.; Poppe, L.; Véniant, M. M., Design and Synthesis of Conformationally Constrained Glucagon-Like Peptide-1 Derivatives with Increased Plasma Stability and Prolonged in Vivo Activity. *J. Med. Chem.* 2008, *51* , 2758-2765.

5. Baggio, L. L.; Drucker, D. J., Biology of Incretins: GLP-1 and GIP. *Gastroenterology* 2007, *132*, 2131-2157.

6. Mentlein, R.; Gallwitz, B.; Schmidt, W. E., Dipeptidyl-peptidase IV hydrolyses gastric inhibitory polypeptide, glucagon-like peptide-1(7–36)amide, peptide histidine methionine and is responsible for their degradation in human serum. *Eur. J. Biochem.* 1993, *214*, 829-835.

7. (a) Meier, J. J., GLP-1 receptor agonists for individualized treatment of type 2 diabetes mellitus. *Nature Reviews Endocrinology* 2012, *8*, 728–742; (b) Nielsen, L. L., Incretin mimetics and DPP-IV inhibitors for the treatment of type 2 diabetes. *Drug Discov. Today* 2005, *10*, 703-

710; (c) Manandhar, B.; Ahn, J.-M., Glucagon-like Peptide-1 (GLP-1) Analogs: Recent Advances, New Possibilities, and Therapeutic Implications. *J. Med. Chem.* 2015, *58*, 1020-1037.

8. (a) de Mello, A. H.; Pra, M.; Cardoso, L. C.; de Bona Schraiber, R.; Rezin, G. T., Incretin-based therapies for obesity treatment. *Metab. Clin and Exp.* 2015, *64*, 967-81. (b) Jackson, V. M.; Breen, D. M.; Fortin, J.-P.; Liou, A.; Kuzmiski, J. B.; Loomis, A. K.; Rives, M.-L.; Shah, B.; Carpino, P. A., Latest approaches for the treatment of obesity. *Exp. Opin. Drug Disc.* 2015, *10* , 825-839. (c) Jackson, V. M.; Price, D. A.; Carpino, P. A., Investigational drugs in Phase II clinical trials for the treatment of obesity: implications for future development of novel therapies. *Exp. Opin. Inv. Drugs* 2014**,** *23* , 1055-1066. (d) Hine, J.; Paterson, H.; Abrol, E.; Russell-Jones, D.; Herring, R., SGLT inhibition and euglycaemic diabetic ketoacidosis. *Lancet Diabetes Endocrinol.* 2015**,** *3*, 503-504.

9. (a) Edmonds, D. J.; Price, D. A., Oral GLP-1 Modulators for the Treatment of Diabetes. In *Ann. Rep. in Med. Chem, Vol 48*, Desai, M. C., Ed. 2013; Vol. 48, pp 119-130; (b) Jones, L. H.; Price, D. A., Medicinal Chemistry of Glucagon-Like Peptide Receptor Agonists. *Prog. Med. Chem., Vol 52* 2013, *52*, 45-96

10. (a) Willard, F. S.; Bueno, A. B.; Sloop, K. W., Small Molecule Drug Discovery at the Glucagon-Like Peptide-1 Receptor. *Exp. Diabetes Res.* 2012. (b) Wootten, D.; Christopoulos, A.; Sexton, P. M., Emerging paradigms in GPCR allostery: implications for drug discovery. *Nat. Rev. Drug Discov.* 2013, *12*, 630-644. (c) Nolte, W. M.; Fortin, J.-P.; Stevens, B. D.; Aspnes, G. E.; Griffith, D. A.; Hoth, L. R.; Ruggeri, R. B.; Mathiowetz, A. M.; Limberakis, C.; Hepworth, D.; Carpino, P. A., A potentiator of orthosteric ligand activity at GLP-1R acts via covalent modification. *Nat. Chem. Biol.* 2014, *10*, 629-634 (d) Cheong, Y.-H.; Kim, M.-K.; Son, M.-H.; Kaang, B.-K., Two small molecule agonists of glucagon-like peptide-1 receptor modulate the

receptor activation response differently. *Biochem. Biophys. Res. Commun.* **2012,** *417* , 558-563; (e) Knudsen, L. B.; Kiel, D.; Teng, M.; Behrens, C.; Bhumralkar, D.; Kodra, J. T.; Holst, J. J.; Jeppesen, C. B.; Johnson, M. D.; de Jong, J. C.; Jorgensen, A. S.; Kercher, T.; Kostrowicki, J.; Madsen, P.; Olesen, P. H.; Petersen, J. S.; Poulsen, F.; Sidelmann, U. G.; Sturis, J.; Truesdale, L.; May, J.; Lau, J., Small-molecule agonists for the glucagon-like peptide 1 receptor. *Proc. Natl. Acad. Sci. U. S. A.* **2007,** *104* , 937-942; (f) Liu, Q.; Li, N.; Yuan, Y.; Lu, H.; Wu, X.; Zhou, C.; He, M.; Su, H.; Zhang, M.; Wang, J.; Wang, B.; Wang, Y.; Na, D.; Ye, Y.; Weiss, H.-C.; Gesing, E. R. F.; Liao, J.; Wang, M.-W., Cyclobutane Derivatives As Novel Nonpeptidic Small Molecule Agonists of Glucagon-Like Peptide-1 Receptor. *J. Med. Chem.* **2012,** *55*, 250-267; (g) Willard, F. S.; Wootten, D.; Showalter, A. D.; Savage, E. E.; Ficorilli, J.; Farb, T. B.; Bokvist, K.; Alsina-Fernandez, J.; Furness, S. G. B.; Christopoulos, A.; Sexton, P. M.; Sloop, K. W., Small molecule allosteric modulation of the glucagon-like peptide-1 receptor enhances the insulinotropic effect of oxyntomodulin. *Mol. Pharmacol.* **2012,** *82*, 1066-1073.

11. (a) Adelhorst, K.; Hedegaard, B. B.; Knudsen, L. B.; Kirk, O., Structure-activity studies of glucagon-like peptide 1. *J. Bio. Chem.* 1994, *269*, 6275-6278; (b) Gallwitz, B.; Witt, M.; Paetzold, G.; Morys-Wortmann, C.; Zimmermann, B.; Eckart, K.; Fölsch, U. R.; Schmidt, W. E., Structure/Activity Characterization of Glucagon-Like Peptide-1. *Eur. J. Biochem.* 1994, *225* , 1151-1156; (c) Parker, J.-C.; Andrews, K. M.; Rescek, D. M.; Massefski Jr, W.; Andrews, G. C.; Contillo, L. G.; Stevenson, R. W.; Singleton, D. H.; Suleske, R. T., Structure-function analysis of a series of glucagon-like peptide 1 analogs. *J. Pept. Res.* 1998, *52*, 398-409.

12 (a) Thornton, K.; Gorenstein, D. G., Structure of Glucagon-Like Peptide(7-36) Amide in a Dodecylphosphocholine Micelle as Determined by 2D NMR. *Biochemistry* 1994, *33*, 3532-3539; (b) Chang, X.; Keller, D.; Bjørn, S.; Led, J. J., Structure and folding of glucagon-like

peptide-1-(7–36)-amide in aqueous trifluoroethanol studied by NMR spectroscopy. *Magn. Reson. Chem.* 2001, *39*, 477-483; (c) Neidigh, J. W.; Fesinmeyer, R. M.; Prickett, K. S.; Andersen, N. H., Exendin-4 and Glucagon-like-peptide-1: NMR Structural Comparisons in the Solution and Micelle-Associated States. *Biochemistry* 2001, *40*, 13188-13200; (d) Andersen, N. H.; Brodsky, Y.; Neidigh, J. W.; Prickett, K. S., Medium-Dependence of the secondary structure of exendin-4 and glucagon-like-peptide-1. *Biorg. Med. Chem.* 2002, *10*, 79-85.

13. (a) Runge, S.; Thøgersen, H.; Madsen, K.; Lau, J.; Rudolph, R., Crystal Structure of the Ligand-bound Glucagon-like Peptide-1 Receptor Extracellular Domain. *J. Biol. Chem.* 2008, *283* , 11340-11347; (b) Underwood, C. R.; Garibay, P.; Knudsen, L. B.; Hastrup, S.; Peters, G. H.; Rudolph, R.; Reedtz-Runge, S., Crystal Structure of Glucagon-like Peptide-1 in Complex with the Extracellular Domain of the Glucagon-like Peptide-1 Receptor. *J. Biol. Chem.* 2010, *285*, 723-730.

14. Siu, F. Y.; He, M.; de Graaf, C.; Han, G. W.; Yang, D.; Zhang, Z.; Zhou, C.; Xu, Q.; Wacker, D.; Joseph, J. S.; Liu, W.; Lau, J.; Cherezov, V.; Katritch, V.; Wang, M.-W.; Stevens, R. C., Structure of the human glucagon class B G-protein-coupled receptor. *Nature* 2013, *499*, 444-449.

15. Murage, E. N.; Gao, G.; Bisello, A.; Ahn, J.-M., Development of Potent Glucagon-like Peptide-1 Agonists with High Enzyme Stability via Introduction of Multiple Lactam Bridges. *J. Med. Chem.* 2010, *53*, 6412-6420.

16. Murage, E. N.; Schroeder, J. C.; Beinborn, M.; Ahn, J.-M., Search for α-helical propensity in the receptor-bound conformation of glucagon-like peptide-1. *Biorg. Med. Chem.* 2008, *16*, 10106-10112.

17. Attramadal, H.; Arriza, J. L.; Aoki, C.; Dawson, T. M.; Codina, J.; Kwatra, M. M.; Snyder, S. H.; Caron, M. G.; Lefkowitz, R. J., Beta-arrestin2, a novel member of the arrestin/beta-arrestin gene family. *J. Biol. Chem.* 1992, *267*, 17882-17890.

18. Kohout, T. A.; Lin, F.-T.; Perry, S. J.; Conner, D. A.; Lefkowitz, R. J., β-Arrestin 1 and 2 differentially regulate heptahelical receptor signaling and trafficking. *Proc. Nat. Acad. of Sci.* 2001, *98*, 1601-1606.

19. Pierce, K. L.; Lefkowitz, R. J., Classical and new roles of [beta]-arrestins in the regulation of G-protein coupled receptors. *Nat. Rev. Neuro.* 2001, *2* , 727-733.

20. Moon, M. J.; Lee, Y.-N.; Park, S.; Reyes-Alcaraz, A.; Hwang, J.-I.; Millar, R. P.; Choe, H.; Seong, J. Y., Ligand Binding Pocket Formed by Evolutionarily Conserved Residues in the Glucagon-like Peptide-1 (GLP-1) Receptor Core Domain. *J. Biol. Chem.* 2015, *290* , 5696-5706

21. Moon, M. J.; Kim, H. Y.; Park, S.; Kim, D.-K.; Cho, E. B.; Park, C. R.; You, D.-J.; Hwang, J.-I.; Kim, K.; Choe, H.; Seong, J. Y., Evolutionarily Conserved Residues at Glucagon-like Peptide-1 (GLP-1) Receptor Core Confer Ligand-induced Receptor Activation. *J. Biol. Chem.* 2012, *287*, 3873-3884.

22. (a) de Araujo, A. D.; Hoang, H. N.; Kok, W. M.; Diness, F.; Gupta, P.; Hill, T. A.; Driver, R. W.; Price, D. A.; Liras, S.; Fairlie, D. P., Comparative α-Helicity of Cyclic Pentapeptides in Water. *Angew. Chem. Int. Ed.* 2014, *53*, 6965-6969; (b) Harrison, R. S.; Shepherd, N. E.; Hoang, H. N.; Beyer, R. L.; Ruiz-Gómez, G.; Kelso, M. J.; Mei Kok, W.; Hill, T. A.; Abbenante, G.; Fairlie, D. P., Helical cyclic pentapeptides constrain HIV-1 Rev peptide for enhanced RNA binding. *Tetrahedron* 2014, *70*, 7645-7650. (c) Harrison, R. S.; Ruiz-Gómez, G.; Hill, T. A.; Chow, S. Y.; Shepherd, N. E.; Lohman, R.-J.; Abbenante, G.; Hoang, H. N.;

Fairlie, D. P., Novel Helix-Constrained Nociceptin Derivatives Are Potent Agonists and Antagonists of ERK Phosphorylation and Thermal Analgesia in Mice. *J. Med. Chem.* 2010, *53*, 8400-8408; (d) Harrison, R. S.; Shepherd, N. E.; Hoang, H. N.; Ruiz-Gomez, G.; Hill, T. A.; Driver, R. W.; Desai, V. S.; Young, P. R.; Abbenante, G.; Fairlie, D. P., Downsizing human, bacterial, and viral proteins to short water-stable alpha helices that maintain biological potency. *Proc. Nat. Acad. Sci. U S A* 2010, *107*, 11686-11691. (e) Shepherd, N. E.; Hoang, H. N.; Abbenante, G.; Fairlie, D. P., Single Turn Peptide Alpha Helices with Exceptional Stability in Water. *J. Am. Chem. Soc.* 2005, *127*, 2974-2983. (f) Shepherd, N. E.; Abbenante, G.; Fairlie, D. P., Consecutive Cyclic Pentapeptide Modules Form Short α-Helices that are Very Stable to Water and Denaturants, *Angew Chem. Int. Edit.* 2004, *43*, 2687-2690. (g) Hoang, H. N.; Driver, R. W.; Beyer, R. L.; Hill, T. A.; de Araujo, A. D.; Plisson, F.; Harrison, R. S.; Goedecke, L.; Shepherd, N. E.; Fairlie, D. P. , Helix nucleation by the smallest known alpha helix in water. *Angew Chem Int Edit* 2016, 55, 8275-8279.

23. Hoang, H. N.; Song, K.; Hill, T. A.; Derksen, D. R.; Edmonds, D. J.; Kok, W. M.; Limberakis, C.; Liras, S.; Loria, P. M.; Mascitti, V.; Mathiowetz, A. M.; Mitchell, J. M.; Piotrowski, D. W.; Price, D. A.; Stanton, R. V.; Suen, J. Y.; Withka, J. M.; Griffith, D. A.; Fairlie, D. P., Short Hydrophobic Peptides with Cyclic Constraints Are Potent Glucagon-like Peptide-1 Receptor (GLP-1R) Agonists. *J. Med. Chem.* 2015, *58*, 4080-4085.

24. (a) Hoang, H. N.; Driver, R. W.; Beyer, R. L.; Malde, A. K.; Le, G. T.; Abbenante, G.; Mark, A. E.; Fairlie, D. P., Protein α-Turns Recreated in Structurally Stable Small Molecules. *Angew. Chem., Int. Ed.* **2011,** *50*, 11107-11111. (b) Shim, S. Y.; Kim, Y.-W.; Verdine, G. L., A New i,i + 3 Peptide Stapling System for α-Helix Stabilization. *Chem. Biol. Drug Des.* **2013,** *82*,

635-642. (c) Kumar, P.; Bansal, M., Dissecting π-helices: sequence, structure and function. *FEBS J*. **2015,** *282*, 4415-4432.

25. Rovo, P.; Farkas, V.; Straner, P.; Szabo, M.; Jermendy, A.; Hegyi, O.; Toth, G. K.; Perczel, A., Rational Design of alpha-Helix-Stabilized Exendin-4 Analogues. *Biochemistry* 2014, *53*, 3540-3552.

26. Hutchinson, E. G.; Thornton, J. M., A revised set of potentials of beta-turn formation in proteins. *Protein Sci*. 1994**,** *3*, 2207-2216.

27. Neumann, J.-M.; Couvineau, A.; Murail, S.; Lacapère, J.-J.; Jamin, N.; Laburthe, M., Class-B GPCR activation: is ligand helix-capping the key? *Trends Biochem. Sci*. 2008, *33* , 314-319.

28. Dong, M.; Te, J. A.; Xu, X.; Wang, J.; Pinon, D. I.; Storjohann, L.; Bordner, A. J.; Miller, L. J., Lactam Constraints Provide Insights into the Receptor-Bound Conformation of Secretin and Stabilize a Receptor Antagonist. *Biochemistry* 2011, *50*, 8181-8192.

29. Zhang, M.; Zhu, Y.; Mu, K.; Li, L.; Lu, J.; Zhao, J.; Huang, X.; Wang, C.; Jia, W., Loss of β-arrestin2 mediates pancreatic-islet dysfunction in mice. *Biochem. Biophys. Res. Commun*. 2013, *435* , 345-349.

30. Luan, B.; Zhao, J.; Wu, H.; Duan, B.; Shu, G.; Wang, X.; Li, D.; Jia, W.; Kang, J.; Pei, G., Deficiency of a β-arrestin-2 signal complex contributes to insulin resistance. *Nature* 2009, *457*, 1146-1149.

31. Larkin, M. A.; Blackshields, G.; Brown, N. P.; Chenna, R.; McGettigan, P. A.; McWilliam, H.; Valentin, F.; Wallace, I. M.; Wilm, A.; Lopez, R.; Thompson, J. D.; Gibson, T. J.; Higgins, D. G., Clustal W and Clustal X version 2.0. *Bioinformatics* 2007, *23*, 2947-2948.

32. Waterhouse, A. M.; Procter, J. B.; Martin, D. M. A.; Clamp, M.; Barton, G. J., Jalview Version 2—a multiple sequence alignment editor and analysis workbench. *Bioinformatics* 2009**,** *25* , 1189-1191.

33. Šali, A.; Blundell, T. L., Comparative Protein Modelling by Satisfaction of Spatial Restraints. *J. Mol. Biol*. 1993**,** *234*, 779-815.

34. Guo, Z.; Mohanty, U.; Noehre, J.; Sawyer, T. K.; Sherman, W.; Krilov, G., Probing the α-Helical Structural Stability of Stapled p53 Peptides: Molecular Dynamics Simulations and Analysis. *Chem. Biol. Drug Design* 2010, *75*, 348-359.

TOC

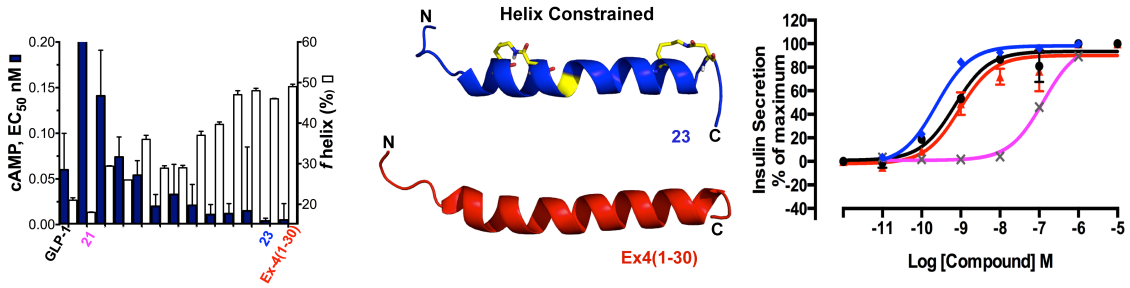
cAMP, EC50 nM
f helix (%)
0.20
0.15
0.10
0.05
0.00
60
50
40
30
20
GLP-1
21
23
Ex-4(1-30)
Helix Constrained
N
C
23
Ex4(1-30)
Insulin Secretion
% of maximum
120
100
80
60
40
20
0
-20
-40
-11
-10
-9
-8
-7
-6
-5
Log [Compound] M